

SYNTHESIS AND RIETVELD REFINEMENT OF AMPHIBOLE ALONG THE JOIN $\text{Ca}_2\text{Mg}_5\text{Si}_8\text{O}_{22}\text{F}_2 - \text{NaCa}_2\text{Mg}_4\text{Ga}_3\text{Si}_6\text{O}_{22}\text{F}_2$

DAVID M. JENKINS

*Department of Geological Sciences and Environmental Studies, Binghamton University,
Binghamton, New York 13902-6000, U.S.A.*

FRANK C. HAWTHORNE

Department of Geological Sciences, University of Manitoba, Winnipeg, Manitoba R3T 2N2

ABSTRACT

Monoclinic amphiboles (a 9.82–9.90, b 18.03–17.99, c 5.27–5.31 Å, β 104.68–105.19°, V 902.5–912.4 Å³, $Z = 2$, $C2/m$) were synthesized along the join $\text{Ca}_2\text{Mg}_5\text{Si}_8\text{O}_{22}\text{F}_2 - \text{NaCa}_2\text{Mg}_4\text{Ga}_3\text{Si}_6\text{O}_{22}\text{F}_2$ at about 1000°C and 3 kbar. The experiments produced fine-grained amphibole with minor quartz, diopside, gallian sapphirine and gallian spinel. The amphibole grains have a nearly equant habit; yields are high (>93 wt%) for all compositions except end-member $\text{NaCa}_2\text{Mg}_4\text{Ga}_3\text{Si}_6\text{O}_{22}\text{F}_2$. Products of synthesis were characterized by electron-microprobe analysis and Rietveld structure-refinement. Using ionized X-ray scattering factors in the Rietveld analysis, we could reproduce the total Ga contents of both the amphiboles and the multiphase mixtures. Gallium occurs at the $M(2)$, $T(1)$ and $T(2)$ sites, and it increases in abundance smoothly along the join; accordingly, the unit-cell parameters and the average bond-distances, notably $\langle T(1)-O \rangle$ and $\langle M(2)-O \rangle$, vary smoothly along the join. The ratio of ^{141}Ga to ^{161}Ga exceeds the 2:1 ratio anticipated for the pargasite-like substitution $\text{Na} + ^{161}\text{Ga} + 2 ^{141}\text{Ga} = \square + ^{161}\text{Mg} + 2 ^{141}\text{Si}$. The current results emphasize the utility of Rietveld analysis for the characterization of fine-grained products of mineral synthesis.

Keywords: synthesis, amphibole, pargasite, Rietveld, gallium, chemical analysis, site populations.

SOMMAIRE

Nous avons synthétisé une série d'amphiboles monocliniques ($9.82 < a < 9.90$, $18.03 < b < 17.99$, $5.27 < c < 5.31$ Å, $104.68 < \beta < 105.19^\circ$, $902.5 < V < 912.4$ Å³, $Z = 2$, $C2/m$) dans l'intervalle de composition $\text{Ca}_2\text{Mg}_5\text{Si}_8\text{O}_{22}\text{F}_2 - \text{NaCa}_2\text{Mg}_4\text{Ga}_3\text{Si}_6\text{O}_{22}\text{F}_2$ à environ 1000°C et 3 kbar. Les produits ont une granulométrie très fine, et l'amphibole y est associée à quartz, diopside, en plus de sapphirine et spinelle enrichis en gallium, tous en proportions mineures. Les grains d'amphibole ont une forme presque idiomorphe; dans tous les cas sauf $\text{NaCa}_2\text{Mg}_4\text{Ga}_3\text{Si}_6\text{O}_{22}\text{F}_2$, l'amphibole constitue plus de 93% du produit de synthèse. Ces produits ont été caractérisés par analyse à la microsonde électronique et par affinement structural selon la méthode de Rietveld. Avec l'utilisation de facteurs de dispersion des rayons X appropriés pour les ions dans l'analyse de Rietveld, nous avons réussi à reproduire la teneur en Ga à la fois de l'amphibole et des mélanges à phases multiples. Le gallium se trouve dans les sites $M(2)$, $T(1)$ et $T(2)$, et augmente en proportion de façon progressive le long de cette série de compositions. De même, les paramètres réticulaires et la longueur moyenne des liaisons, notamment $\langle T(1)-O \rangle$ et $\langle M(2)-O \rangle$, varient de façon progressive dans l'intervalle de composition étudié. Le rapport de ^{141}Ga à ^{161}Ga dépasse 2:1, la valeur anticipée selon un schéma de substitution pargasitique, $\text{Na} + ^{161}\text{Ga} + 2 ^{141}\text{Ga} = \square + ^{161}\text{Mg} + 2 ^{141}\text{Si}$. Nos résultats soulignent l'utilité d'une analyse par la méthode de Rietveld pour caractériser les produits de synthèse à granulométrie fine.

Mots-clés: synthèse, amphibole, pargasite, Rietveld, gallium, analyse chimique, population des sites.

INTRODUCTION

The Al content of calcic amphiboles has received considerable attention in recent years because of its correlation with metamorphic grade in metamafic rocks (e.g., Laird & Albee 1981) and with pressure in granitic rocks (e.g., Hammarstrom & Zen 1986). Most

field studies and experimental calibrations of the variation of the Al content in amphiboles as a function of pressure (P) and temperature (T) have dealt with the bulk content of Al and not with its distribution among the sites in the amphibole structure. This latter information is critical for the formulation of thermodynamic activity–composition relationships and for

the determination of the extent to which disorder involving Al contributes to the configurational entropy of aluminous amphiboles. The two principal factors responsible for the paucity of such information by single-crystal X-ray-diffraction techniques are (1) the very small grain-size (typically $2 \times 5 \mu\text{m}$ in plan view) of amphiboles produced in experimental studies, and (2) the similarity in X-ray scattering factors of Al, Mg, and Si.

The present study examines the behavior of Ga in amphiboles along the join $\text{Ca}_2\text{Mg}_5\text{Si}_8\text{O}_{22}\text{F}_2(\text{F-Tr}) - \text{NaCa}_2\text{Mg}_4\text{Ga}_3\text{Si}_6\text{O}_{22}\text{F}_2(\text{F-Ga-Prg})$. This compositional join represents the substitution of Na, ^{61}Ga , and ^{44}Ga into tremolitic amphibole by the pargasite-like exchange $\text{Na} + ^{61}\text{Ga} + 2 ^{44}\text{Ga} = \square + ^{61}\text{Mg} + 2 ^{44}\text{Si}$, which is a 1:1 combination of the Ga-tschermaks exchange $^{61}\text{Ga} + ^{44}\text{Ga} = ^{61}\text{Mg} + ^{44}\text{Si}$ and Ga-edenite exchange $\text{Na} + ^{44}\text{Ga} = \square + ^{44}\text{Si}$. In this study, we use Ga as an analogue for Al, with the advantage that Ga ($Z = 31$) scatters X rays much more strongly than Al ($Z = 13$), and hence can be distinguished from Mg ($Z = 12$) and Si ($Z = 14$) *via* X-ray scattering. The Rietveld technique uses the entire powder-diffraction pattern to derive various instrumental and structure parameters by minimizing the difference between the observed and calculated pattern *via* least-squares refinement. Rietveld structure-refinement was first applied to synthetic amphiboles by Raudsepp *et al.* (1987); however, this work was complicated by the occurrence of ternary site-populations (*e.g.*, Mg, Sc, Al) because only part of the Al was replaced by another trivalent cation. In the present work, we have replaced both octahedrally and tetrahedrally coordinated Al by Ga, and hence avoid this problem; all octahedral and tetrahedral site-populations are binary.

This study also provides a test of the Rietveld technique for the determination of mineral compositions because independent compositional constraints are placed on both the bulk composition of the crystalline assemblage (composition of the starting mixture) and the composition of the amphibole crystals (electron-

microprobe analysis).

EXPERIMENTAL PROCEDURE

Techniques of synthesis

All amphiboles were synthesized from mixtures of reagent-grade Na_2CO_3 , CaCO_3 , MgO , Ga_2O_3 , SiO_2 , and CaF_2 prepared in 20 mol% increments along the F-Tr - F-Ga-Prg join. Starting mixtures were loaded into $\text{Ag}_{50}\text{Pd}_{50}$ capsules and roasted in air from 500–600°C to drive off any adsorbed H_2O , but not all CO_2 from the carbonates, prior to sealing. Syntheses were done at the conditions listed in Table 1 using internally heated pressure vessels with Ar as the pressure medium. Further details of the experimental apparatus are described in Lykins & Jenkins (1992). The products of synthesis are quite hard and compact, but seem completely crystalline, and contain high yields of amphibole (minimum of 86 wt%). The samples were first ground manually for several minutes in a corundum mortar and pestle and then with a mechanical mortar and pestle for about 15 minutes.

X-ray diffraction

Powder X-ray diffraction step-scans were obtained on a Philips PW1700 diffractometer operated at 40 kV and 40 mA. The goniometer is of the Bragg-Brentano type, equipped with a diffracted-beam graphite monochromator at the scintillation detector. Intensities were collected from 9 to 100° 2θ at 0.1° steps for counting times of 4–6 seconds to give about 3000–4000 counts on the strongest peaks. Fixed divergence and receiving slits of $\frac{1}{2}^\circ$ were used. The powdered sample was mounted in a $15 \times 20 \times 1$ mm rectangular aluminum holder backed by a glass plate. The surface of the sample was roughed up slightly with beam-parallel striations using a razor blade, as discussed in Raudsepp *et al.* (1990), in order to help ensure random orientation of grains.

TABLE 1. BULK COMPOSITIONS AND CONDITIONS OF SYNTHESIS ALONG THE JOIN $\text{Ca}_2\text{Mg}_5\text{Si}_8\text{O}_{22}\text{F}_2 - \text{NaCa}_2\text{Mg}_4\text{Ga}_3\text{Si}_6\text{O}_{22}\text{F}_2$

Run Code	Bulk composition	T (°C)	P (kbar)	t (h)	Products*
TREM 19-3	$\text{Ca}_2\text{Mg}_5\text{Si}_8\text{O}_{22}\text{F}_2$	998(10)	2.96(5)	70	Amph, Qtz
PARG 10-1	$\text{Na}_{0.2}\text{Ca}_2\text{Mg}_{4.8}\text{Ga}_{0.6}\text{Si}_{7.6}\text{O}_{22}\text{F}_2$	1000(10)	3.03(5)	96	Amph, Qtz
PARG 9-1	$\text{Na}_{0.4}\text{Ca}_2\text{Mg}_{4.6}\text{Ga}_{1.2}\text{Si}_{7.2}\text{O}_{22}\text{F}_2$	975(25)	3.02(5)	94	Amph, Qtz, Spr1
PARG 8-2	$\text{Na}_{0.6}\text{Ca}_2\text{Mg}_{4.4}\text{Ga}_{1.8}\text{Si}_{6.8}\text{O}_{22}\text{F}_2$	1000(10)	2.92(5)	65	Amph, Qtz, Spr1, Di
PARG 7-1	$\text{Na}_{0.8}\text{Ca}_2\text{Mg}_{4.2}\text{Ga}_{2.4}\text{Si}_{6.4}\text{O}_{22}\text{F}_2$	1000(10)	3.20(5)	100	Amph, Spr1, Di
PARG 6-4	$\text{NaCa}_2\text{Mg}_4\text{Ga}_3\text{Si}_6\text{O}_{22}\text{F}_2$	1000(10)	2.95(5)	122	Amph, Spr2, Di, Spl

*Abbreviations: Amph = amphibole; Di = diopside; Qtz = quartz; Spr1 and Spr2 = gallian sapphirine (see text); Spl = gallian spinel

Electron-microprobe analysis

Electron-microprobe analysis of amphibole was done at the University of Manitoba using a Cameca SX-50 operated at 15 kV and 20 nA current *via* wavelength-dispersion spectrometry (WDS). The samples were dispersed in epoxy and loaded into cylinders drilled into a Lucite disk, cured, and polished with a final grit of 0.3 μm diameter. The standards used were albite for Na, diopside for Ca and Si, olivine for Mg, either $\text{Ga}_5\text{Gd}_3\text{O}_{12}$, Ga_2O_3 , or NaGaSiO_4 for Ga, and fluor-riebeckite for F. Identical results were obtained for Ga regardless of the Ga standard used. Despite the small grain-sizes (1–2 μm diameter) and attendant uncertainties concerning the presence of subsurface grain contamination (*e.g.*, Graham *et al.* 1989), acceptable compositions could be obtained using the criteria that the analytical total be 90 wt% or higher, and the sum of all cations less Na be 15.0 ± 0.2 apfu (atoms per formula unit).

Electron-microprobe analysis of the gallian sapphirine phases in some of the run products was done at Binghamton University using a JEOL 8900 operated at 15 kV and 10 nA *via* WDS. The extremely small grain-size of these particles required dispersal of the grains on polished graphite stubs to ensure that free-standing grains could be identified for analysis. The standards used were albite for Na, diopside for Ca, SiO_2 for Si, MgO for Mg, GaP for Ga, and apatite for F. Analytical totals were generally less than 100 wt% because the small size of the grains ensured that the excitation volume of the beam was larger than the volume of the grain. We accepted compositions with analytical totals of 70 wt% or higher and cation totals of 14.0 ± 0.2 apfu, as these gave reasonable stoichiometries for a sapphirine-structure phase.

Rietveld structure-refinement

Rietveld refinement was done with the program DBWS-9006 (Wiles & Young 1981, Young 1993) because of its ability to refine four phases simultaneously. The following refinement sequence was used: (1) zeropoint of 2θ , (2) scale factor of amphibole, (3) four terms (B_m) for the background intensity, y_{bi} , in the expression

$$y_{bi} = \sum_{m=0}^5 B_m [(2\theta_i/2\theta_0) - 1]^m,$$

where $2\theta_0$ is the origin of the background polynomial, (4) unit-cell parameters, (5) peak full-width-at-half-maximum (FWHM) parameters U, V, and W in the expression of Caglioti *et al.* (1958), (6) first term (NA) in the pseudo-Voigt profile-function mixing-parameter expression $\eta = \text{NA} + \text{NB}(2\theta)$, (7) atomic coordinates of all atoms in amphibole, (8) the parameter P in the asymmetry factor $A = 1 - \text{P}[\text{sign}(2\theta_1 - 2\theta_K) (2\theta_1 - 2\theta_K)^2 / \tan\theta_K]$ for peaks below 50° , (9) overall

displacement factor (B) for amphibole, (10) one or two terms (G_i) in the Rietveld–Toraya preferred orientation factor $P_K = [G_2 + (1 - G_2)\exp(-G_1\alpha^2_K)]$, (11) the second term NB in the pseudo-Voigt mixing-parameter expression, (12) the site occupancies of all tetrahedral and octahedral sites and the M(4) site in amphibole, and (13) the scale factors of any additional phases. Isotropic displacement factors for each atom in amphibole were based on those used by Raudsepp *et al.* (1987) for synthetic pargasitic amphibole and were held constant throughout the refinement. For the minor phases, the peak FWHM parameters were set equal to those of the amphibole (based on initial single-phase refinements), the pseudo-Voigt mixing parameter η was set equal to 0.5, the asymmetry, preferred orientation and overall displacement factors were set to 0, and all of these terms were held constant thereafter during the refinement. All variables in items 1–13 above were allowed to vary in the final cycles of all refinements.

The relative effects of the asymmetry factor, overall displacement factor, and preferred orientation terms for the Bragg reflections of amphibole were assessed by comparing refinements made with and without these terms. Deletion of the preferred orientation term G_1 was found to have the greatest influence on the agreement indices (*e.g.*, 1–2% increase in R_B) and caused slight shifts in the atomic coordinates and cation site-occupancies. The overall displacement factor (B) and peak-asymmetry factor had very minor effects on the agreement indices (*e.g.*, 0.1–0.2% increase in R_B) and virtually no effect on any of the structural parameters of amphibole or site occupancies. The deletion of any one of these terms from a given refinement did not cause a significant ($>1\sigma$) change in the results; the inclusion of all of these terms in the final refinement produced the best overall

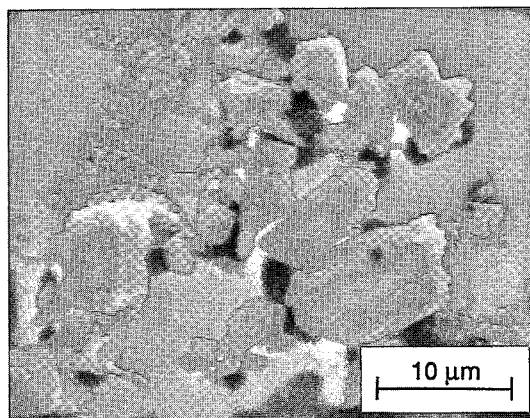


FIG. 1. SEM photograph of PARG 9-1 showing the typical blocky habit of amphibole grown along the join $\text{Ca}_2\text{Mg}_5\text{Si}_8\text{O}_{22}\text{F}_2 - \text{NaCa}_2\text{Mg}_4\text{Ga}_3\text{Si}_6\text{O}_{22}\text{F}_2$.

fit to the pattern (best agreement indices) while retaining realistic unit-cell parameters, interatomic distances, etc.

The use of ionized *versus* neutral X-ray scattering factors makes a significant difference to the refined site-populations (Della Ventura *et al.* 1993). As part of this work, we examined this point in some detail by doing our refinements with both ionized and neutral scattering factors. As discussed below, ionized scattering factors gave much superior results, and all data given here are for refinements with ionized scattering factors.

To test that a global minimum was reached in the refinement procedure, several refinements were done with very different starting occupancies; Ga was distributed over all available tetrahedral and octahedral sites, and also was initially placed at the *T*(2) and *M*(1) sites. In all cases, the same final site-occupancies were obtained.

RESULTS

Products of synthesis

Except for the F–Tr end-member, the grain shapes encountered along the join are quite blocky (Fig. 1) and produced X-ray-diffraction patterns with minimal effects attributed to preferred orientation. The F–Tr end-member produced crystals that are more elongate, and consequently the diffraction pattern has minor enhancement of the *hk0* reflections. Attempts to synthesize hydroxyl- rather than fluorine-bearing gallium-pargasite were unsuccessful.

The presence of minor additional phases in the synthesis of amphibole is typical of many studies (*e.g.*, Jenkins 1987, Graham *et al.* 1989, Raudsepp *et al.*

TABLE 3. AGREEMENT INDICES* AND AMPHIBOLE PATTERN PARAMETERS** FROM MULTI-PHASE RIETVELD REFINEMENTS USING IONIZED SCATTERING FACTORS

	TREM 19-3	PARG 10-1	PARG 9-1	PARG 8-2	PARG 7-188	PARG 6-4
R_p	10.1	8.1	9.3	8.3	7.9(6)	8.4
R_{wp}	13.6	10.9	12.5	11.3	10.7(7)	11.4
R_{exp}	8.4	6.5	7.7	6.3	7.0(6)	7.3
GOF	1.62	1.68	1.62	1.79	1.53	1.56
$R_p(\text{Amph})$	6.1	5.3	6.4	5.7	5.6(3)	5.4
$R_p(\text{Di})$	--	--	--	17.6	13(3)	11.8
$R_p(\text{Qtz})$	16.3	16.9	15.4	17.5	--	--
$R_p(\text{Spr1})$	--	--	27.7	18.5	17(2)	--
$R_p(\text{Spr2})$	--	--	--	--	--	11.8
$R_p(\text{Spl})$	--	--	--	--	--	8.9
U	0.10(2)	0.15(2)	0.10(2)	0.11(2)	0.18(2)	0.31(5)
V	-0.13(2)	-0.09(2)	-0.06(2)	-0.07(2)	-0.10(2)	-0.15(3)
W	0.072(4)	0.046(3)	0.033(3)	0.045(4)	0.038(7)	0.048(6)
NA	0.35(5)	0.65(5)	0.66(3)	0.60(7)	0.75(4)	0.77(9)
NB	0.04(1)	0.02(1)	--	0.002(2)	0.001(1)	0.001(2)
P	0.23(4)	0.19(4)	0.49(8)	0.15(7)	0.4(2)	0.11(8)
B	-0.38(9)	-0.04(8)	0.07(9)	-0.1(1)	-0.1(2)	-0.2(1)
C_1	-1.3(4)	-0.08(1)	-0.18(2)	-0.10(1)	-0.12(4)	-0.12(2)
C_2	0.68(2)	--	--	--	--	--
ΔW_{Df}	1.4	1.2	1.4	1.0	1.3(1)	1.2
σ_{int}	1.4	1.6	1.4	1.6	1.58(5)	1.5
Zerpoint§	0.101(2)	-0.004(2)	0.037(2)	0.020(2)	0.01(3)	-0.006(2)

* $R_p = 100 \sum |y_i - y_{calc}| / \sum y_i$, $R_{wp} = 100 \sum (y_i - y_{calc})^2 / \sum y_i^2$, $R_{exp} = 100 \{(N - P) / \sum y_i\}^{1/2}$, GOF = Goodness-of-fit = R_{wp} / R_p , $R_p = 100 \sum |I_o - I_c| / \sum I_o$, where y_i and y_{calc} are the observed and calculated intensities at the *i*th step, $w_i = 1/y_i$, N = total number of steps, P = number of parameters being refined, I_o and I_c are the observed and calculated intensities for the Bragg reflections of each phase.

**U, V, W = FWHM peak profile parameters; NA, NB = pseudo-Voigt profile-function mixing-parameters; P = asymmetry parameter; B = overall displacement factor; C_1 , C_2 = preferred orientation terms

†DWD = Durbin-Watson d statistic (Hill & Flack 1987)

‡FWHM = multiplicity factor for all e.s.d.'s according to the algorithm of Béjar & Lelann (1991); calculated but not applied here

§Zerpoint = zerpoint of 2θ

§§Average and 1 σ uncertainty (in parentheses) for four different refinements

1991), including this one (Table 1). Aside from devoting considerable effort to determine the compositional region in which 100% yields can be obtained (*e.g.*, Jenkins 1987, Pawley *et al.* 1993), one can use the Rietveld technique to derive the structural parameters of the dominant phase, so long as the minor phases can be adequately characterized. Of the minor phases encountered in this study, namely diopside ($\text{CaMgSi}_2\text{O}_6$), quartz (SiO_2), gallian sapphirine, and gallian spinel (MgGa_2O_4), only gallian sapphirine displays much variation in composition. Microprobe analysis showed that the gallian sapphirine phases in PARG 9-1, 8-2 and 7-1 have essentially the same composition ($\text{Mg}_{3.75}\text{Ca}_{0.60}\text{Ga}_{7.05}\text{Si}_{2.60}\text{O}_{20}$: Spr1), whereas that in PARG 6-4 was found to be markedly higher in Ca and lower in Mg ($\text{Mg}_{2.85}\text{Ca}_{1.55}\text{Ga}_{7.30}\text{Si}_{2.30}\text{O}_{20}$: Spr2). High levels of Ca in (natural aluminous) sapphirine is rare; however, syntheses done in this study along the join $\text{Mg}_4\text{Ga}_8\text{Si}_2\text{O}_{20}$ – $\text{Mg}_2\text{Ca}_2\text{Ga}_8\text{Si}_2\text{O}_{20}$ at 1000°C and 3.1 kbar show that nearly pure yields of synthetic sapphirine are possible for these bulk compositions. This agrees with the wide compositional range reported for Ga-rich synthetic sapphirine (Smart & Glasser 1978, Barbier 1990). Chemical compositions of amphibole synthesized in this study are given in Table 2.

Rietveld refinement: amphibole

Agreement indices and various pattern-statistics for the Rietveld refinements of this study are given in

TABLE 2. CHEMICAL COMPOSITIONS OF SYNTHETIC AMPHIBOLE

Oxide	TREM 19-3	PARG 10-1	PARG 9-1	PARG 8-2	PARG 7-1	PARG 6-4
*n =	5	6	7	6	5	4
SiO_2	58.1(10)	52.2(11)	48.7(13)	45.0(6)	42.3(16)	41.4(3)
Ga_2O_3	0.0	7.1(11)	12.6(5)	17.5(13)	20.9(13)	24.4(8)
MgO	25.0(11)	23.0(6)	22.1(4)	20.7(6)	18.8(13)	17.7(10)
CaO	13.2(3)	12.9(2)	12.3(2)	12.3(3)	12.0(7)	11.4(4)
Na_2O	0.0	0.82(13)	1.52(8)	2.30(14)	2.7(2)	3.4(2)
F	4.4(4)	4.2(3)	3.7(3)	4.2(3)	4.0(7)	4.4(2)
Total	100.7(14)	100.2(18)	100.9(10)	102.0(14)	100.7(14)	102.7(5)
-O = F	-1.8	-1.8	-1.5	-1.8	-1.7	-1.8
Total	98.9(14)	98.4(18)	99.4(18)	100.2(13)	99.0(14)	100.9(4)
Si	7.96	7.48	7.08	6.76	6.56	6.45
⁶⁹ Ga	0.0	0.52	0.92	1.24	1.44	1.55
sum T	7.96	8.00	8.00	8.00	8.00	8.00
⁶⁹ Ga	0.0	0.13	0.26	0.44	0.64	0.89
⁶⁷ Mg	5.00	4.87	4.74	4.56	4.34	4.11
sum C	5.00	5.00	5.00	5.00	4.98	5.00
⁶⁹ Mg	0.10	0.04	0.05	0.08	0.00	0.00
Ca	1.94	1.98	1.92	1.98	1.99	1.90
sum B	2.04	2.02	1.97	2.06	1.99	1.90
Na	0.0	0.23	0.43	0.67	0.81	1.03
F	1.9	1.9	1.7	2.0	2.0	2.2

*n = number of point analyses

TABLE 4. UNIT-CELL PARAMETERS FOR AMPHIBOLE (C2/m) FROM MULTI-PHASE RIETVELD REFINEMENT OF PRODUCTS OF SYNTHESIS IN TABLE 1

	F-TREM*	TREM 19-3	PARG 10-1	PARG 9-1	PARG 8-2	PARG 7-1**	PARG 6-4
a (Å)	9.787(3)	9.8182(6)	9.8356(6)	9.8620(6)	9.8820(7)	9.897(2)	9.8992(9)
b (Å)	18.004(2)	18.032(1)	18.025(1)	18.025(1)	18.017(1)	18.010(2)	17.992(2)
c (Å)	5.263(2)	5.2699(4)	5.2801(3)	5.2930(4)	5.2990(4)	5.3059(9)	5.3081(6)
β (°)	104.44(2)	104.680(4)	104.793(4)	104.924(5)	105.068(5)	105.165(3)	105.190(6)
V (Å ³)	898.1(5)	902.5(1)	905.0(1)	909.2(1)	911.0(1)	912.8(2)	912.4(2)

* From Cameron & Gibbs (1973); ** Average of four refinements

Table 3. The refined unit-cell parameters, atomic coordinates, selected interatomic distances, and cation site-occupancies for amphibole are given in Tables 4, 5, 6 and 7, respectively. Initial refinements gave very small negative occupancies of Ga at the M(4) site; consequently, the Ga content at the M(4) site was fixed at zero. The results reported for fluor-tremolite (TREM 19-3) were calculated with nominal site-populations, and may be compared directly with the results of Cameron & Gibbs (1973).

*Rietveld refinement:
minor phases and whole pattern*

Refinement of minor phases was done using the structural data of Lager *et al.* (1982) for quartz, Levina & Prewitt (1981) for diopside, and Hill *et al.* (1979) for gallian spinel. In the absence of a detailed structural analysis of the gallian sapphirine phases encountered in this study, the following approach was taken. Preliminary Rietveld refinement of single-phase sap-

TABLE 5. ATOMIC COORDINATES FROM RIETVELD REFINEMENTS

atom	F-TREM*	TREM 19-3	PARG 10-1	PARG 9-1	PARG 8-2	PARG 7-1**	PARG 6-4
O(1)							
x	0.1126(3)	0.1181(16)	0.1143(18)	0.1135(21)	0.1108(21)	0.1092(18)	0.1127(29)
y	0.0847(2)	0.0863(7)	0.0849(7)	0.0867(9)	0.0879(10)	0.0873(8)	0.0902(14)
z	0.2179(6)	0.2153(29)	0.2123(29)	0.2164(38)	0.2033(39)	0.2066(30)	0.2099(53)
O(2)							
x	0.1187(3)	0.1183(17)	0.1164(19)	0.1102(21)	0.1126(22)	0.1132(10)	0.1062(30)
y	0.1702(2)	0.1697(8)	0.1698(8)	0.1735(10)	0.1717(11)	0.1723(11)	0.1716(15)
z	0.7239(6)	0.7272(29)	0.7231(29)	0.7288(35)	0.7326(37)	0.7295(16)	0.7263(51)
O(3)							
x	0.1020(4)	0.1005(16)	0.1001(16)	0.1027(19)	0.1026(21)	0.1036(24)	0.1005(28)
y	0	0	0	0	0	0	0
z	0.7124(8)	0.7060(34)	0.7105(33)	0.7125(43)	0.7083(47)	0.7232(28)	0.7283(62)
O(4)							
x	0.3644(4)	0.3565(15)	0.3570(16)	0.3519(19)	0.3516(21)	0.3554(25)	0.3524(28)
y	0.2484(2)	0.2447(7)	0.2457(8)	0.2479(9)	0.2470(10)	0.2477(11)	0.2462(14)
z	0.7907(7)	0.7884(32)	0.7822(32)	0.7776(42)	0.7749(48)	0.7868(36)	0.7795(62)
O(5)							
x	0.3471(3)	0.3432(19)	0.3474(21)	0.3516(26)	0.3552(25)	0.3541(25)	0.3552(31)
y	0.1351(2)	0.1321(7)	0.1338(8)	0.1370(10)	0.1384(11)	0.1395(2)	0.1389(15)
z	0.1001(7)	0.0961(33)	0.0933(37)	0.0886(46)	0.0935(48)	0.1080(45)	0.1015(69)
O(6)							
x	0.3444(3)	0.3489(19)	0.3451(21)	0.3456(26)	0.3397(27)	0.3423(19)	0.3419(33)
y	0.1197(2)	0.1161(7)	0.1166(8)	0.1155(10)	0.1155(11)	0.1148(6)	0.1129(15)
z	0.5857(6)	0.5911(36)	0.5963(42)	0.6055(53)	0.6192(54)	0.6284(17)	0.6166(72)
O(7)							
x	0.3408(5)	0.3445(20)	0.3451(22)	0.3483(25)	0.3517(28)	0.3455(24)	0.3530(36)
y	0	0	0	0	0	0	0
z	0.2922(10)	0.2880(43)	0.2899(41)	0.2935(53)	0.2901(59)	0.2637(25)	0.2676(78)
T(1)							
x	0.2829(1)	0.2844(9)	0.2847(9)	0.2857(10)	0.2835(9)	0.2836(14)	0.2829(12)
y	0.0834(1)	0.0833(4)	0.0846(4)	0.0847(4)	0.0848(4)	0.0853(3)	0.0849(5)
z	0.2960(2)	0.3058(19)	0.3026(17)	0.3056(20)	0.3027(19)	0.3044(15)	0.3065(24)
T(2)							
x	0.2900(1)	0.2900(11)	0.2893(11)	0.2898(13)	0.2897(13)	0.2906(23)	0.2889(17)
y	0.1707(1)	0.1699(4)	0.1709(4)	0.1699(5)	0.1711(5)	0.1720(6)	0.1720(6)
z	0.8041(2)	0.8005(20)	0.8044(20)	0.8065(24)	0.8139(25)	0.8166(21)	0.8127(31)
M(1)							
x	0	0	0	0	0	0	0
y	0.0885(1)	0.0896(7)	0.0871(7)	0.0858(9)	0.0862(9)	0.0860(4)	0.0854(12)
z	1/2	1/2	1/2	1/2	1/2	1/2	1/2
M(2)							
x	0	0	0	0	0	0	0
y	0.1760(1)	0.1762(7)	0.1775(7)	0.1786(7)	0.1781(7)	0.1786(5)	0.1783(8)
z	0	0	0	0	0	0	0
M(3)							
x	0	0	0	0	0	0	0
y	0	0	0	0	0	0	0
z	0	0	0	0	0	0	0
M(4)							
x	0	0	0	0	0	0	0
y	0.2771(1)	0.2759(4)	0.2773(5)	0.2784(6)	0.2785(6)	0.2789(7)	0.2799(8)
z	1/2	1/2	1/2	1/2	1/2	1/2	1/2
A							
x	--	--	0	0	0	0	0
y	--	--	1/2	1/2	1/2	1/2	1/2
z	--	--	0	0	0	0	0

Isotropic displacement factors: O(1)-O(4) = 0.8; O(5)-O(6) = 1.0; O(7) = 1.2; T(1)-T(2) = 0.4; M(1)-M(3) = 0.6; M(4) = 0.9; A = 2.3 Å²

* From Cameron & Gibbs (1973); ** Average of four refinements

TABLE 6. SELECTED INTERATOMIC DISTANCES (Å) FOR REFINED SYNTHETIC AMPHIBOLE

	F-TREM*	TREM 19-3	PARG 10-1	PARG 9-1	PARG 8-2	PARG 7-1**	PARG 6-4
T(1)-O(1)	1.614(3)	1.58(2)	1.62(2)	1.64(2)	1.65(2)	1.67(1)	1.63(3)
T(1)-O(5)	1.628(3)	1.63(2)	1.65(2)	1.74(3)	1.75(3)	1.70(2)	1.74(4)
T(1)-O(6)	1.630(4)	1.59(2)	1.61(2)	1.64(3)	1.71(3)	1.75(2)	1.67(4)
T(1)-O(7)	1.606(2)	1.62(1)	1.64(1)	1.66(1)	1.68(1)	1.69(1)	1.71(2)
<T(1)-O>	1.620	1.61	1.63	1.67	1.70	1.70	1.69
T(2)-O(2)	1.623(3)	1.63(2)	1.64(2)	1.71(2)	1.69(2)	1.70(2)	1.74(3)
T(2)-O(4)	1.587(3)	1.51(2)	1.52(2)	1.56(2)	1.53(2)	1.53(2)	1.50(3)
T(2)-O(5) ^a	1.648(4)	1.66(2)	1.63(2)	1.58(2)	1.57(3)	1.62(2)	1.62(4)
T(2)-O(6)	1.659(3)	1.68(2)	1.67(2)	1.64(3)	1.60(3)	1.61(1)	1.67(4)
<T(2)-O>	1.629	1.62	1.62	1.62	1.60	1.61	1.63
M(1)-O(1)x2	2.059(3)	2.12(2)	2.11(2)	2.09(2)	2.14(2)	2.12(2)	2.13(3)
M(1)-O(2)x2	2.054(4)	2.04(2)	2.06(2)	2.11(2)	2.10(2)	2.11(1)	2.07(3)
M(1)-O(3)x2	2.057(3)	2.05(1)	2.03(1)	2.02(2)	2.02(2)	2.05(1)	2.05(2)
<M(1)-O>	2.057	2.07	2.06	2.08	2.08	2.09	2.08
M(2)-O(1)x2	2.146(4)	2.14(2)	2.16(2)	2.16(2)	2.09(2)	2.11(2)	2.08(3)
M(2)-O(2) ^b x2	2.077(3)	2.07(2)	2.08(2)	2.01(2)	2.02(2)	2.04(1)	2.01(3)
M(2)-O(4) ^c x2	2.024(4)	2.11(2)	2.10(2)	2.09(2)	2.12(2)	2.06(2)	2.11(3)
<M(2)-O>	2.082	2.11	2.11	2.09	2.08	2.07	2.07
M(3)-O(1)x4	2.055(3)	2.09(1)	2.05(1)	2.08(2)	2.06(2)	2.06(1)	2.11(2)
M(3)-O(3) ^d x2	2.011(4)	2.04(2)	2.02(2)	2.03(2)	2.06(3)	2.00(2)	1.95(3)
<M(3)-O>	2.040	2.08	2.04	2.07	2.06	2.04	2.06
M(4)-O(2)x2	2.400(4)	2.40(2)	2.40(2)	2.35(2)	2.40(2)	2.39(1)	2.38(3)
M(4)-O(4) ^e x2	2.308(3)	2.35(2)	2.33(2)	2.37(2)	2.36(3)	2.39(2)	2.38(3)
M(4)-O(5) ^f x2	2.756(3)	2.83(2)	2.79(2)	2.75(2)	2.71(2)	2.65(1)	2.66(3)
M(4)-O(6) ^g x2	2.514(2)	2.57(2)	2.58(2)	2.59(2)	2.66(3)	2.67(1)	2.66(3)
<M(4)-O>	2.495	2.53	2.53	2.52	2.53	2.52	2.52

^a x, y, 1+z; ^b x, y, -1+z; ^c 1/2-x, 1/2-y, 1-z; * From Cameron & Gibbs (1973); ** Average of four refinements

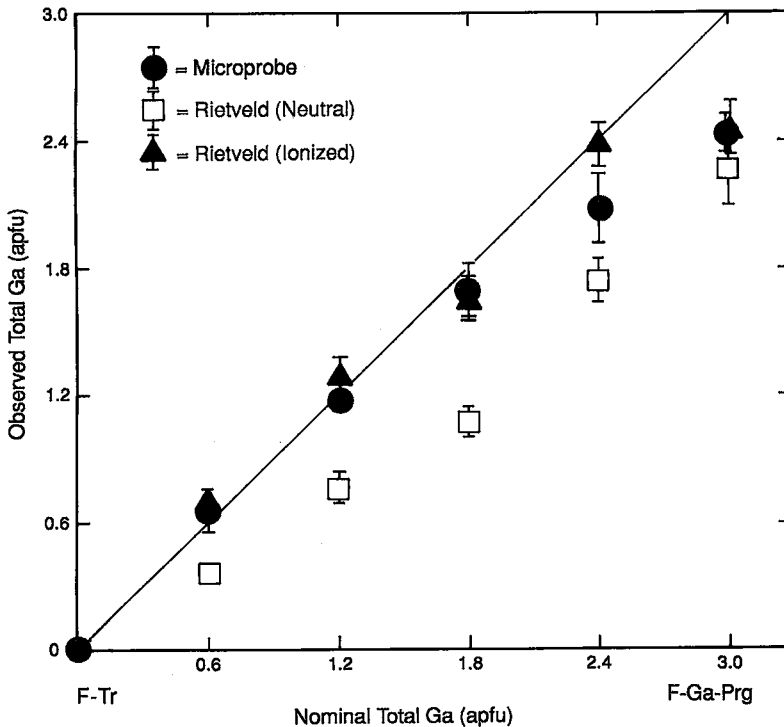


FIG. 2. Total Ga atoms per formula unit (apfu) in amphiboles by electron-microprobe analysis (circles) and Rietveld refinement [using neutral (squares) and ionized (triangles) scattering factors] plotted against the nominal total Ga content. The diagonal line shows one-to-one correspondence between observed and nominal Ga contents.

phirine synthesized along the join $Mg_4Ga_8Si_2O_{20} - Mg_2Ca_2Ga_8Si_2O_{20}$ showed that they are the triclinic 1A (formerly 1Tc) polytype with the *PI* structure (Merlino 1980), rather than the monoclinic 2M polytype with the *P2₁/a* structure (Moore 1969). Owing to their structural complexity and minor abundance, it was not possible to obtain adequate results for any structural data except the unit-cell parameters. Thus the gallian sapphirine phases in the synthesis products (Spr1 and Spr2) were modeled using the 1A structure and cation distribution reported by Merlino (1980), with Ga instead of Al and Ca occurring at the largest octahedral sites. The unit-cell parameters for Spr1 were then refined from the PARG 7-1 X-ray patterns, in which Spr1 is most abundant, using initial cell-parameters provided by J. Barbier (pers. comm., 1992), and holding all but the scale factors of the other phases constant. The resulting cell-parameters for Spr1 are a 10.258(8), b 10.619(17), c 8.782(15) Å, α 107.0(3), β 95.5(1), γ 124.1(1)°. These unit-cell parameters were used for the Spr1 in PARG 9-1 and PARG 8-2 without further refinement because of the very low abundance of gallian sapphirine in these run products. The cell parameters for Spr2 were refined from the X-ray pattern of PARG 6-4: a 10.373(5), b 10.773(6), c 8.925(5) Å, α 106.09(6), β 95.83(6), γ 124.45(6)°.

DISCUSSION

Choice of scattering curves

All Rietveld refinements were done with both neutral and ionized scattering curves in order to determine the more accurate procedure of refinement. First, the structure of Ga-free fluor-tremolite (TREM 19-3) was refined with the *M*(1,2,3) and *T*(1,2) site-scattering expressed as (Mg,Ga) and (Si,Ga), respectively, and considered as variable. Neutral scattering factors produced slightly negative Ga-occupancies (1-5%) at all *M*(1,2,3) and *T*(1,2) sites; ionized scattering factors produced zero Ga-occupancies at *M*(1,2,3) and *T*(1), and slightly positive ($4 \pm 1\%$) Ga-occupancy at *T*(2). Second, for the Ga-bearing amphiboles, the total Ga-content derived from the sum of the refined site-populations can be compared with the values derived by electron-microprobe analysis and with the nominal Ga values; this is done in Figure 2. It is immediately apparent that there is close agreement between the Rietveld and electron-microprobe values for ionized scattering curves; for neutral scattering curves, the Rietveld-refined Ga-contents fall way below the electron-microprobe values and the nominal values.

The Rietveld refinements show clearly that ionized scattering curves give accurate bulk compositions

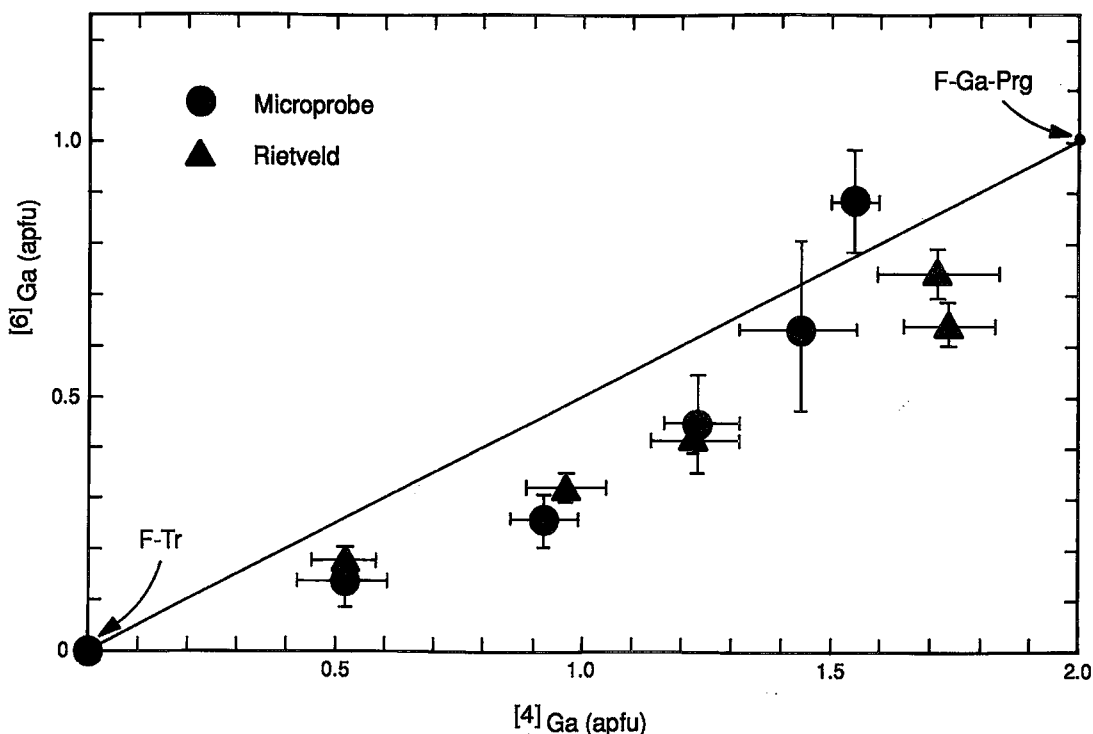


FIG. 3. Proportion of ^{160}Ga and ^{144}Ga (apfu) in amphibole from electron-microprobe data (circles) and Rietveld refinement (triangles) results.

TABLE 7. REFINED POPULATIONS OF TETRAHEDRAL AND OCTAHEDRAL SITES IN AMPHIBOLE*

	TREM 19-3	PARG 10-1	PARG 9-1	PARG 8-2	PARG 7-1**	PARG 6-4
T(1) Si	4.0	3.55(5)	3.23(6)	2.94(6)	2.67(6)	2.70(9)
Ga	0.0	0.45(5)	0.77(6)	1.06(6)	1.33(6)	1.30(9)
T(2) Si	4.0	3.93(5)	3.80(6)	3.83(7)	3.59(8)	3.58(9)
Ga	0.0	0.07(5)	0.20(6)	0.17(3)	0.41(8)	0.42(9)
M(1) Mg	2.0	1.97(2)	1.95(3)	1.98(3)	1.99(4)	1.96(5)
Ga	0.0	[0.03(2)]	[0.05(3)]	[0.02(3)]	[0.01(4)]	[0.04(5)]
M(2) Mg	2.0	1.83(2)	1.68(3)	1.58(3)	1.56(3)	1.56(5)
Ga	0.0	0.17(2)	0.32(3)	0.42(3)	0.54(3)	0.74(5)
M(3) Mg	1.0	1.02(2)	0.98(2)	0.98(2)	0.97(1)	0.98(3)
Ga	0.0	[-0.02(2)]	[0.02(2)]	[0.02(2)]	[0.03(1)]	[0.02(3)]
M(4) Ca	1.92(6)	1.91(7)	1.79(9)	1.96(10)	1.76(10)	1.73(12)
Mg	0.08(6)	0.09(7)	0.21(9)	0.04(10)	0.24(10)	0.27(12)
A Na	0.0	0.27(2)	0.46(3)	0.71(3)	0.80(1)	0.86(5)
Σ Ga (obs.)	0.0	0.69(7)	1.29(8)	1.65(10)	2.38(10)	2.46(13)
Σ Ga (EPMA)	0.0	0.66(9)	1.18(5)	1.69(13)	2.08(17)	2.43(9)
Σ Ga (nom.)	0.0	0.60	1.20	1.80	2.40	3.00

* Numbers in square brackets are considered zero in the total Ga summation. Units: atoms per formula unit; ** Average of four refinements.

(and, presumably, site populations). This is in accord with the work of Della Ventura *et al.* (1993) for synthetic amphibole of richteritic composition.

Comparison of nominal and analyzed amphibole compositions

Inspection of Figure 2 shows that both the Rietveld and electron-microprobe Ga content of the synthetic amphibole compositions agree with the nominal values for all except the most Ga-rich (Ga = 3.0 apfu) composition. We emphasize that electron-microprobe analysis and Rietveld refinement provide completely independent assessments of the Ga content; the close agreement is strong evidence for the reliability of both sets of results, and indicates the reliability of the Rietveld technique for accurately determining the abundance of a strong X-ray-scattering species. Both the Rietveld and electron-microprobe results indicate that the amphibole synthesized from the most Ga-rich bulk composition (PARG 6-4) failed to obtain its full complement of Ga (the remaining Ga residing in other phases), and may indicate that the saturation limit of Ga substitution has been reached at these P-T conditions.

Ordering of Ga in the amphibole structure

The content of ^{44}Ga and ^{61}Ga in amphibole is shown in Figure 3, in which the microprobe compositions from Table 2 (circles) are compared to Rietveld compositions from Table 7 (triangles). The agreement between the two techniques is quite good at low levels of Ga, but deviates somewhat at the highest Ga content, where Rietveld refinement indicates a higher proportion of ^{44}Ga than does the microprobe analysis. Figure 3 shows that the amphiboles in PARG 7-1 and PARG 6-4 have nearly identical Ga contents, and supports the hypothesis that they are essentially saturated in Ga. However, there are significant differences in the unit-cell dimensions of these two amphiboles. There is

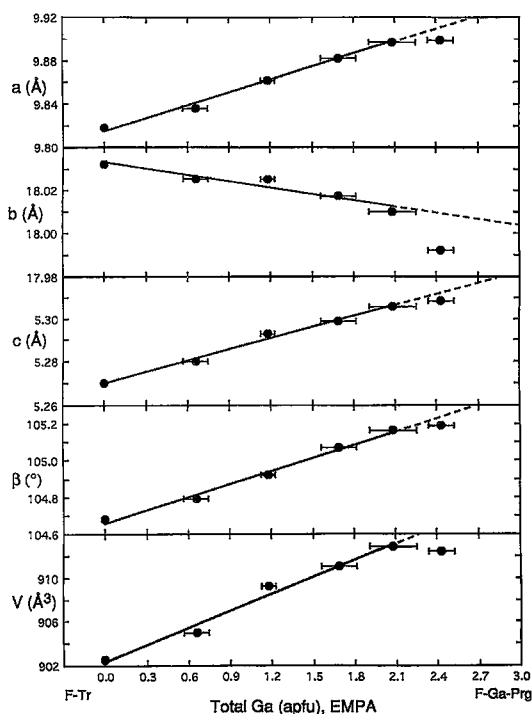


FIG. 4. Unit-cell parameters for amphiboles synthesized in this study. Standard deviations are smaller than the symbols.

a significant decrease in the *b* dimension and increases in *a* and *c*, indicating a higher $^{61}\text{Ga}/^{44}\text{Ga}$ in PARG 6-4 than in PARG 7-1. This is shown to be the case by the refined Ga site-occupancies (Table 7); both PARG 7-1 and PARG 6-4 have ~ 1.73 ^{44}Ga apfu, whereas they have 0.64 and 0.74 ^{61}Ga apfu, respectively. Thus the tetrahedra seem to saturate with Ga before the octahedra.

Unit-cell parameters

The variation in unit-cell parameters as a function of Ga content is shown in Figure 4. The behavior of the individual cell-edges is unusual, and reflects the two different substitutions involving Ga: substitution of Ga for Mg decreases the size of the octahedral strip, whereas substitution of Ga for Si increases the size of the double chain of tetrahedra. The combined effect of these two substitutions is an increase in cell volume with increasing total Ga-content (Fig. 4). There is a suggestion of nonlinearity in the variation of cell volume, with higher Ga contents having slightly lower volumes than linear extrapolation would suggest. This could result from an increase in the $^{61}\text{Ga}/^{44}\text{Ga}$ ratio

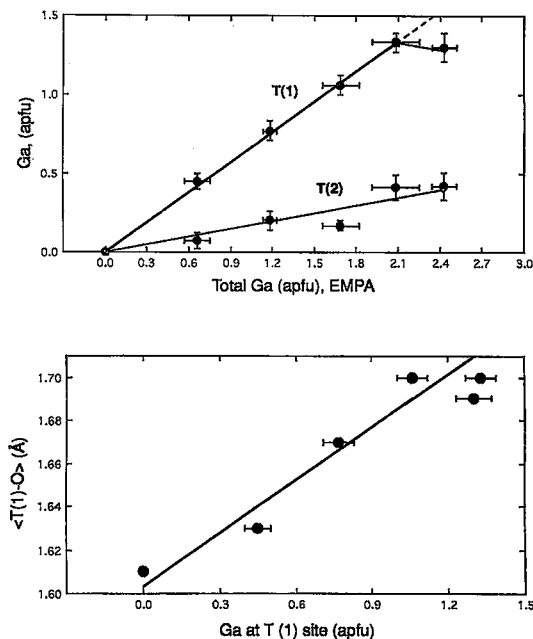


Fig. 5. ^{14}Ga (apfu) (top) and average $T(1)\text{-O}$ bond distances (bottom) for the amphiboles synthesized in this study.

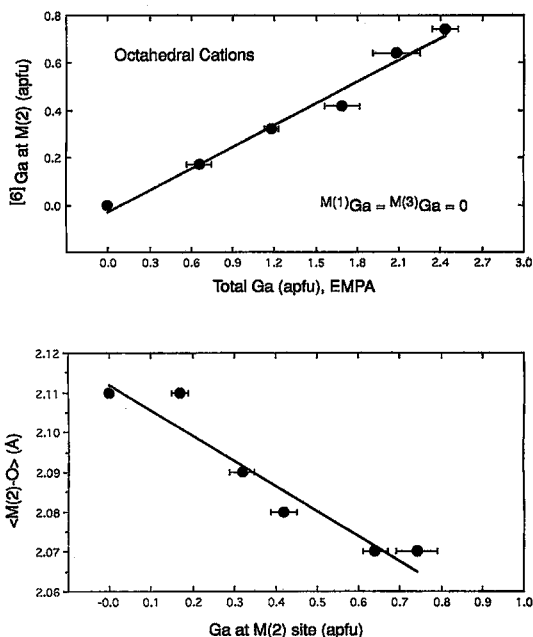


Fig. 6. ^{6}Ga (apfu) (top) and average $M(2)\text{-O}$ bond-distances (bottom) for the amphiboles synthesized in this study.

at higher Ga content, because, as discussed above (Fig. 3), ^{6}Ga is favored by higher total-Ga content.

It is well established (Colville *et al.* 1966) that the b dimension in amphiboles is very sensitive to the mean radius of the cations at the $M(2)$ site. As shown by site-scattering refinement (Table 7), ^{6}Ga is completely ordered at $M(2)$, and thus the effect of increasing ^{6}Ga is to cause a decrease in the b dimension. Conversely, increasing ^{14}Ga increases the mean size of the tetrahedrally coordinated cations, producing two different effects. First, the length of the double chain increases, thus increasing the c dimension (Fig. 4). Second, the tetrahedra of the double-chain also rotate [*via* change in the $O(5)\text{-O}(6)\text{-O}(5)$ angle], and in order for the $M(4)$ cation to maintain its bond-valence requirements with regard to the $O(5)$ and $O(6)$ anions (see discussion in Hawthorne 1983), the back-to-back double chains shear relative to each other, causing significant changes in the β angle and the a dimension.

The ^{14}Ga site-populations (apfu) and $\langle T(1)\text{-O} \rangle$ bond-distances are shown in Figure 5. Gallium is strongly ordered at the $T(1)$ site, consistent with the general assignment of tetrahedrally coordinated Al to the $T(1)$ site in calcic amphiboles (Hawthorne 1983). About 20% of the ^{14}Ga occurs at the $T(2)$ site. There is a linear increase in $\langle T(1)\text{-O} \rangle$ with increasing Ga content that is commensurate with the difference in size between $^{14}\text{Ga}^{3+}$ (0.47 Å) and $^{14}\text{Si}^{4+}$ (0.26 Å) (ionic radii from Shannon 1976). There is no signifi-

cant increase in $\langle T(2)\text{-O} \rangle$ because of the relatively low level of Ga at this site and because of the large standard deviations for the bond distances. The plateaus in the $T(1)$ [and $T(2)$?] Ga contents and in the $\langle T(1)\text{-O} \rangle$ distances at high total-Ga content again suggest Ga saturation in the tetrahedra in these compositions of amphibole.

All of the octahedrally coordinated Ga occurs at the $M(2)$ site (Fig. 6); there is no significant Ga at the $M(1)$ and $M(3)$ sites. There is a small but significant decrease in the $\langle M(2)\text{-O} \rangle$ distance with increasing Ga content of $M(2)$, reflecting the substitution of $^{6}\text{Ga}^{3+}$ (0.62 Å) for $^{6}\text{Mg}^{2+}$ (0.72 Å).

Na at the A site

There is good agreement between the Na content at the A site refined by the Rietveld method and that

TABLE 8. WEIGHT PERCENTAGES OF PHASES PRESENT, AND COMPARISON OF THE NOMINAL (BULK) TOTAL Ga_2O_3 CONTENT TO THAT CALCULATED FROM THE RIETVELD SCALE-FACTORS AND PHASE COMPOSITIONS

Phase	TREM 19-3	PARG 10-1	PARG 9-1	PARG 8-2	PARG 7-1*	PARG 6-4
Amph	99(3)	98(3)	97(3)	93(4)	94.0(8)	86(4)
Qtz	0.90(6)	1.48(9)	1.8(1)	2.1(1)	—	—
Di	—	—	—	2.1(3)	1.6(2)	2.3(3)
Spn1	—	—	1.4(2)	3.2(2)	4.9(3)	—
Spn2	—	—	—	—	—	10.5(3)
Spl	—	—	—	—	—	1.2(1)
Refined Ga_2O_3	0.0	7.4(7)	14.0(8)	17.7(8)	23.3(10)	28.8(9)
Nominal Ga_2O_3	0.0	6.64	12.83	18.58	23.99	29.04

* Average of four refinements

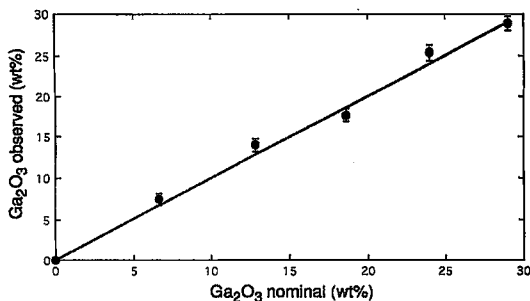


FIG. 7. Bulk Ga_2O_3 content of each synthesis mixture determined by Rietveld analysis *versus* nominal Ga_2O_3 .

observed by microprobe analysis (*cf.* Tables 2, 7). In fact, the lower Na-content for the amphibole in PARG 6-4 obtained by Rietveld refinement is more in line with the apparent saturation of the amphibole in Ga at a level commensurate with the amphibole in PARG 7-1, marking the cessation of any Na substitution coupled with Ga substitution. In view of the artificially high concentrations one often obtains for elements of low-atomic number from electron-microprobe analysis of small particles (*e.g.*, Newbury 1984), the Na content obtained from Rietveld refinement may prove more reliable.

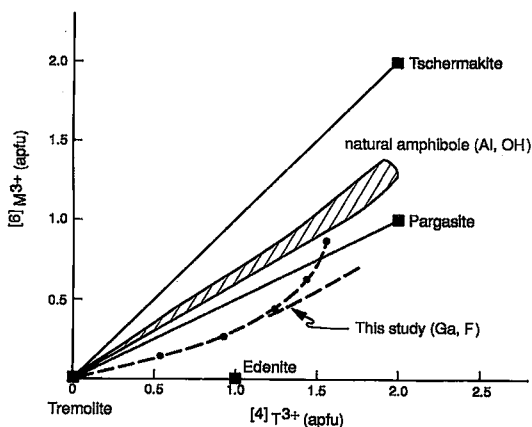


FIG. 8. Proportion of octahedrally coordinated trivalent cations (M^{3+}) *versus* tetrahedrally coordinated trivalent cations (T^{3+}) in calcic amphiboles; the general trend observed for natural (aluminous, hydroxyl-bearing) calcic amphiboles is shown by the shaded area, and the trend observed here for gallium-fluor-amphibole is shown by dashed lines. Note the split at high T^{3+} values between the trend from electron-microprobe results (dash-dot curve) and Rietveld (dashed curve) analysis.

Nominal versus observed bulk Ga-contents

A distinct advantage of the Rietveld technique is that one can easily quantify the relative proportions of crystalline phases present in a mixture from the refined unit-cell volumes, chemical compositions, and the scale factor of each phase (*e.g.*, Hill & Howard 1987, Snyder & Bish 1989). In this study, we can check on the overall performance of the Rietveld method by comparing the refined total Ga-content with the nominal Ga-content of the mixture, as these values were determined by completely independent methods. Table 8 shows the weight percentages of the phases present in each mixture, along with the bulk Ga_2O_3 content as weighed and as derived from Rietveld refinement. As shown in Figure 7, the agreement is excellent, being within the precision of the Rietveld technique.

Comparison with aluminous pargasite

Gallium orders strongly at the $T(1)$ and $M(2)$ sites, with a small (but significant) amount of Ga at the $T(2)$ site. As a result, the proportion of tetrahedrally coordinated to octahedrally coordinated trivalent cations is greater than is usually the case for natural calcic amphibole. Figure 8 shows the compositions of tschermakite [$\text{Ca}_2\text{Mg}_3\text{Al}_4\text{Si}_6\text{O}_{22}(\text{OH})_2$], pargasite [$\text{NaCa}_2\text{Mg}_4\text{Al}_3\text{Si}_6\text{O}_{22}(\text{OH})_2$], edenite [$\text{NaCa}_2\text{Mg}_5\text{AlSi}_7\text{O}_{22}(\text{OH})_2$], and tremolite [$\text{Ca}_2\text{Mg}_5\text{Si}_8\text{O}_{22}(\text{OH})_2$] on a graph of $[4]T^{3+}$ *versus* $[6]M^{3+}$. The trend observed in this study is shown by the dash-dot (microprobe) and dashed (Rietveld) curves; the split in the Ga-amphibole curve is due to the small difference between cation site-assignments from the microprobe and Rietveld results, as discussed above (Fig. 3). In contrast, natural (Al,OH) calcic amphiboles tend to lie in the shaded zone (Fig. 8) between the tschermakite-tremolite and pargasite-tremolite joins (*e.g.*, Doolan *et al.* 1978, Schumacher 1991). The relatively high proportion of tetrahedrally coordinated trivalent cations may be facilitated by the presence of F rather than OH at the O(3) site, as suggested by the relative ease of synthesizing fluor-edenite *versus* (hydroxy-)edenite (Raudsepp *et al.* 1991).

Our results have two main implications for the distribution of Al in the crystal structure of natural calcic amphiboles. First, octahedrally coordinated Al is expected to be strongly ordered at the $M(2)$ site. This is generally the case in natural amphiboles, both calcic, sodic-calcic, and alkali amphiboles (Hawthorne 1983). However, Oberti *et al.* (1995a) have shown that Al also occurs at $M(3)$ in natural pargasitic amphibole. Infrared spectroscopic results (Raudsepp *et al.* 1987) also show Al to be partly disordered over the octahedrally coordinated sites in synthetic pargasite. However, in synthetic fluor-pargasite, with $[6]M^{3+} = \text{Cr}^{3+}$, Ga, and Sc, the $[6]M^{3+}$ cations order at the $M(2)$

site (Raudsepp *et al.* 1987). Hence the behavior of the gallium-fluor-pargasite synthesized here parallels that of the synthetic fluor-pargasite crystals of Raudsepp *et al.* (1987). These results suggest that the identity of the O(3) anion is a major factor in the ordering of M^{3+} over the $M(1,2,3)$ sites, the M^{3+} cations tending to order more strongly at $M(2)$ where F is present at O(3). This may be a trivalent analogue of the well-known Fe-F avoidance principle (Rosenberg & Foit 1977). Second, tetrahedrally coordinated Al is expected to strongly order at the $T(1)$ site, but with some Al at the $T(2)$ site. This agrees with the study of Oberti *et al.* (1995b), who showed that ^{27}Al can partly disorder over the $T(1)$ and $T(2)$ sites in amphibole depending on the thermal history.

CONCLUSIONS

In this study, the Rietveld technique proved very effective at characterizing both the amphiboles and the minor phases in the mixtures under investigation. In synthetic gallium-fluor-pargasite, Ga is strongly ordered at the $M(2)$ and $T(1)$ sites, with a small, but significant, amount of Ga at the $T(2)$ site. Although the amphiboles investigated here serve as only approximate analogues for natural calcic amphiboles, they provide a valuable basis for comparison and useful insight into the substitution of trivalent cations in the amphibole structure. Such information will assist in the larger task of thermodynamically modeling these substitutions as a function of P, T, and mineral assemblage. The overall success of the Rietveld method in this study further demonstrates the utility of this technique in characterizing fine-grained products of mineral synthesis.

ACKNOWLEDGEMENTS

This research was funded by National Science Foundation grant EAR-9104266 to DMJ and NSERC Major Equipment, Operating, and Infrastructure grants to FCH. We thank Mati Raudsepp for his advice and help with many aspects of this study, Ron Chapman (UM) and Bill Blackburn (BU) for assistance with the electron-microprobe analyses, Michael Fleet for kindly donating the NaGaSiO_4 sample, and Jacques Barbier for providing approximate unit-cell dimensions for the gallian sapphirine phases encountered here. Discussions with Peter Burns and Neil Ball were very helpful with various aspects of this study. Constructive reviews by R.N. Abbott, Jr., and an anonymous reviewer were greatly appreciated. Thanks go to Anne Hull for drafting the figures.

REFERENCES

- BARBIER, J. (1990): $\text{Mg}_4\text{Ga}_4\text{Ge}_2\text{O}_{20}$: A new synthetic analog of the mineral sapphirine. *Phys. Chem. Minerals* **17**, 246-252.
- BÉRAR, J.F. & LELANN, P. (1991): E.S.D.'s and estimated probable error obtained in Rietveld refinements with local correlations. *J. Appl. Crystallogr.* **24**, 1-5.
- CAGLIOTTI, G., PAOLETTI, A. & RICCI, F.P. (1958): Choice of collimators for a crystal spectrometer for neutron diffraction. *Nucl. Instrum.* **3**, 223-228.
- CAMERON, M. & GIBBS, G.V. (1973): The crystal structure and bonding of fluor-tremolite: A comparison with hydroxyl tremolite. *Am. Mineral.* **58**, 879-888.
- COLVILLE, P.A., ERNST, W.G. & GILBERT, M.C. (1966): Relationships between cell parameters and chemical compositions of monoclinic amphiboles. *Am. Mineral.* **51**, 1727-1754.
- DELLA VENTURA, G., ROBERT, J.-L., BÉNY, J.-M., RAUDSEPP, M. & HAWTHORNE, F.C. (1993): The OH-F substitution in Ti-rich potassium richterite: Rietveld structure refinement and FTIR and micro-Raman spectroscopic studies of synthetic amphiboles in the system $\text{K}_2\text{O}-\text{Na}_2\text{O}-\text{CaO}-\text{MgO}-\text{SiO}_2-\text{TiO}_2-\text{H}_2\text{O}-\text{HF}$. *Am. Mineral.* **78**, 980-987.
- DOOLAN, B.L., ZEN, E-AN & BENCE, A.E. (1978): Highly aluminous hornblendes: compositions and occurrences from southwestern Massachusetts. *Am. Mineral.* **63**, 1088-1099.
- GRAHAM, C.M., MARESCH, W.V., WELCH, M.D. & PAWLEY, A.R. (1989): Experimental studies on amphiboles: a review with thermodynamic perspectives. *Eur. J. Mineral.* **1**, 535-555.
- HAMMARSTROM, J.M. & ZEN, E-AN (1986): Aluminum in hornblende: an empirical igneous geobarometer. *Am. Mineral.* **71**, 1297-1313.
- HAWTHORNE, F.C. (1983): The crystal chemistry of the amphiboles. *Can. Mineral.* **21**, 173-480.
- HILL, R.J., CRAIG, J.R. & GIBBS, G.V. (1979): Systematic of the spinel structure type. *Phys. Chem. Minerals.* **4**, 317-339.
- & FLACK, H.D. (1987): The use of the Durbin-Watson d statistic in Rietveld analysis. *J. Appl. Crystallogr.* **20**, 356-361.
- & HOWARD, C.J. (1987): Quantitative phase analysis from neutron powder diffraction data using the Rietveld method. *J. Appl. Crystallogr.* **20**, 467-474.
- JENKINS, D.M. (1987): Synthesis and characterization of tremolite in the system $\text{H}_2\text{O}-\text{CaO}-\text{MgO}-\text{SiO}_2$. *Am. Mineral.* **72**, 707-715.
- LAGER, G.A., JORGENSEN, J.D. & ROTELLA, F.J. (1982): Crystal structure and thermal expansion of α -quartz SiO_2 at low temperatures. *J. Appl. Phys.* **53**, 6751-6756.
- LAIRD, J. & ALBEE, A.L. (1981): High pressure metamorphism of mafic schist from northern Vermont. *Am. J. Sci.* **281**, 97-126.

- LEVIEN, L. & PREWITT, C.T. (1981): High-pressure structural study of diopside. *Am. Mineral.* **66**, 315-323.
- LYKINS, R.W. & JENKINS, D.M. (1992): Experimental determination of pargasite stability relations in the presence of orthopyroxene. *Contrib. Mineral. Petrol.* **112**, 405-413.
- MERLINO, S. (1980): Crystal structure of sapphirine – 1Tc. *Z. Kristallogr.* **151**, 91-100.
- MOORE, P.B. (1969): The crystal structure of sapphirine. *Am. Mineral.* **54**, 31-49.
- NEWBURY, D.E. (1984): Microbeam analysis of samples of unusual shape. *J. Phys. (Paris)* **45(C2)**, 775-780.
- OBERTI, R., HAWTHORNE, F.C., UNGARETTI, L. & CANNILLO, E. (1995a): ⁶¹Al disorder in amphiboles from mantle peridotites. *Can. Mineral.* **33**, (in press).
- _____, UNGARETTI, L., CANNILLO, E., HAWTHORNE, F.C. & MEMMI, I. (1995b): Temperature-dependent Al order-disorder in the tetrahedral double-chains of C2/m amphiboles. *Eur. J. Mineral.* (in press).
- PAWLEY, A.R., GRAHAM, C.M. & NAVROTSKY, A. (1993): Tremolite-richterite amphiboles: synthesis, compositional and structural characterization, and thermochemistry. *Am. Mineral.* **78**, 23-35.
- RAUDSEPP, M., HAWTHORNE, F.C. & TURNOCK, A.C. (1990): Evaluation of the Rietveld method for the characterization of fine-grained products of mineral synthesis: the diopside-hedenbergite join. *Can. Mineral.* **28**, 93-109.
- _____, TURNOCK, A.C. & HAWTHORNE, F. C. (1991): Amphibole synthesis at low pressure: what grows and what doesn't. *Eur. J. Mineral.* **3**, 983-1004.
- _____, _____, _____, SHERRIFF, B.L. & HARTMAN, J.S. (1987): Characterization of synthetic pargasitic amphiboles (NaCa₂Mg₄M³⁺Si₆Al₂O₂₂(OH,F)₂; M³⁺= Al, Cr, Ga, Sc, In) by infrared spectroscopy, Rietveld structure refinement, and ²⁷Al, ²⁹Si, and ¹⁹F MAS NMR spectroscopy. *Am. Mineral.* **72**, 580-593.
- ROSENBERG, P.E. & FOIT, F.F., JR. (1977): Fe²⁺ – F avoidance in silicates. *Geochim. Cosmochim. Acta* **41**, 345-346.
- SCHUMACHER, R. (1991): Compositions and phase relations of calcic amphiboles in epidote- and clinopyroxene-bearing rocks of the amphibolite and lower granulite facies, central Massachusetts, USA. *Contrib. Mineral. Petrol.* **108**, 196-211.
- SHANNON, R.D. (1976): Revised effective ionic radii and systematic studies of interatomic distances in halides and chalcogenides. *Acta Crystallogr.* **A32**, 751-767.
- SMART, R.M. & GLASSER, F.P. (1978): Phase formation in the system MgO–Ga₂O₃–SiO₂. *J. Mat. Sci.* **13**, 671-674.
- SNYDER, R.L. & BISH, D.L. (1989): Quantitative analysis. In *Modern Powder Diffraction* (D.L. Bish & J.E. Post, eds.). *Rev. Mineral.* **20**, 101-144.
- WILES, D.B. & YOUNG, R.A. (1981): A new computer program for Rietveld analysis of X-ray powder diffraction patterns. *J. Appl. Crystallogr.* **14**, 149-151.
- YOUNG, R.A. (1993): Introduction to the Rietveld method. In *The Rietveld Method* (R.A. Young, ed.). Oxford Univ. Press, Oxford, U.K. (39-42).

Received January 4, 1994, revised manuscript accepted May 25, 1994.